Feature-based evaluation of a wearable surface EMG sensor against laboratory standard EMG during force-varying and fatiguing contractions.

Emer P. Doheny, *Member, IEEE*, Cathy Goulding, Matthew W. Flood, Lara McManus and Madeleine M. Lowery, *Member, IEEE*

***Abstract* — Recent advances in wearable sensors enable recording of electromyography (EMG) outside the laboratory for extended periods of time. However, the properties of wearable EMG systems designed for long-term recording may differ from those of laboratory-standard systems, potentially impacting data. This study evaluated EMG features derived from signals recorded using a wearable system (BioStampRC, MC10 Inc.) against a reference laboratory system (Bagnoli, Delsys Inc.). Surface EMG data from the biceps brachii were recorded simultaneously using both systems during isometric elbow flexion, between 10% and 80% of maximum voluntary contraction (MVC), and during sustained submaximal fatiguing contraction, in twelve subjects. Linear and nonlinear EMG temporal and spectral features were then compared across both systems. No effect of recording system was detected on EMG onset/offset times, or on the relationship between force and EMG root mean squared amplitude. However, the relationships between force and median frequency, percentage determinism and multiscale entropy differed between systems. Baseline noise was also greater for the BioStampRC. Lower median frequencies were observed for the wearable system, likely due to the larger interelectrode distance, however, the relative change in EMG amplitude and median frequency during the fatiguing contraction was similar for both. Percentage determinism increased and multiscale entropy decreased during the fatiguing contraction for both systems, with higher and lower values respectively for the wearable system. Results indicate that the BiostampRC is appropriate for EMG onset/offset and amplitude estimation. However, caution is advised when comparing across systems as spectral and nonlinear features may differ due to electrode design differences.**

***Index Terms*—EMG validation; wearable sensors; median frequency; determinism; multiscale entropy**

I. Introduction

ELECTROMYOGRAPHY (EMG) data have traditionally been recorded in a laboratory setting, assessing muscle activity over relatively short periods of time, in an unnatural environment. Laboratory surface EMG systems typically are not portable, costly to purchase and wired. Recent developments in wearable sensors may provide an alternative solution, enabling continuous long-term monitoring of muscle activity beyond the laboratory [1]–[6].

The BioStampRC (MC10 Inc., MA, USA) is one of the first of a new generation of wearable EMG sensors suitable for long-term recording. Unlike other wearable EMG systems which included wiring between the electrodes and amplifier unit [5], [6], the BioStampRC is completely wireless. It is small, soft and flexible and does not constrain natural body motions, enabling it to be worn during the day and at night. It is also waterproof, has a long battery life (≈ 28 hours), and on-board memory. Previous studies have examined the capabilities of the BioStampRC in long term electrocardiography monitoring [7], as an accelerometer for gait and postural sway analysis in persons with multiple sclerosis [8], and for home-based monitoring of patients with Parkinson's and Huntington's disease [9]. Surface EMG applications of this sensor have recently begun to be explored, with only limited data reported to date [10]–[12]. The surface EMG signal is more complex and spans a broader frequency range than accelerometry or electrocardiography signals. However, EMG signals recorded by the BioStampRC have yet to be comprehensively validated against a laboratory standard surface EMG system. A well validated wearable EMG system would enable long-term remote monitoring of muscle function in any location, with wide-ranging clinical applications such as movement analysis in individuals with neuromuscular disorders [2] or following musculoskeletal surgery [10], detection of muscle fatigue during physical exercise [13], biofeedback during physical rehabilitation [14] or EMG-based control of external devices [15].

Guidelines for surface EMG sensors and sensor placement were published in 1999 as an output of the SENIAM consortium project [16] and have been widely accepted as the best-practice for recording traditional bipolar surface EMG. However, due to recent advances in sensor technology,

This manuscript was received on 19 December 2018. This work was supported in part by Science Foundation Ireland under grant number SFI/RC/2289 and the European Research Council under the grant number ERC-2014-CoG-646923. *(Corresponding Author: E.P. Doheny)*

E.P. Doheny (e-mail: emer.doheny@ucd.ie), C. Goulding, M.W. Flood, L. McManus and M.M. Lowery are with the Department of Electrical and Electronic Engineering, University College Dublin, Dublin, Ireland.

E.P. Doheny, M.W. Flood and M.M. Lowery are also with the Insight Centre for Data Analytics, University College Dublin, Dublin, Ireland.

including wearable sensors and high-density electrode arrays, EMG sensor design for novel applications has begun to deviate from these guidelines. Truly wireless and wearable sensors, that can record EMG data continuously over several days or weeks without requiring battery recharging or frequent data uploading, may require compromises in terms of hardware design, electrode configuration or data sampling. In the case of substantial differences in parameters such as sampling rate, memory storage requirements, circuit design, inter-electrode distance, and the physical size and weight of electrodes, it is necessary to validate wearable EMG sensors against reference laboratory systems before the data can be reliably interpreted.

During dynamic contractions and functional tasks, EMG activity is commonly used to determine muscle onset and offset times [17]. EMG amplitude and power spectrum features, such as the median frequency, are widely used to provide information on muscle activation level and changes associated with muscle fatigue [18], [19]. Changes in the structure of the surface EMG signal can also be identified through the use of nonlinear methods including recurrence analysis and measures of signal entropy [20], [21]. While the influence of electrode configuration, has been established through experimental and modeling studies [22]–[27], the sensitivity of all of these features to specific software and hardware design choices relevant to wearable sensors is not clear.

The aim of this study was, therefore, to evaluate features of EMG signals recorded using the wearable BioStampRC EMG sensor. To achieve this, commonly used features of surface EMG signals recorded using BioStampRC were compared with those obtained using a standard wired bipolar surface EMG sensor (Bagnoli, Delsys Inc., MA, USA) during isometric contractions across a range of force levels and during sustained fatiguing contraction. The results demonstrated that while estimates of relative changes in EMG amplitude and muscle onset/offset times detected using the BiostampRC are comparable to those estimated using conventional surface EMG, spectral and nonlinear signal features differed between the two.

II. Methods

A. Participants

Twelve healthy subjects (6 female, 6 male; aged 25.68 ± 10.23 years (mean ± SD); age range 22-58 years; median age 23 years) with no history of neuromuscular disorders provided their informed consent and volunteered to participate in this study. Ethical approval was obtained from the Human Research Ethics Committee at University College Dublin.

B. Set up

Subjects were seated in a comfortable chair, with their right elbow flexed to 90 degrees and their upper arm vertical next to the trunk, Fig. 1. The forearm was held in a neutral position to limit pronation/supination [28] and inside a cuff which was connected to a load cell. The load cell (SM-500N Interface Inc., Scottsdale, AZ, USA) was placed beneath the wrist to measure elbow flexion force. Subjects were provided with visual feedback using Spike2 software (Cambridge Electronic Design Ltd, Cambridge, UK).

Surface EMG data were collected simultaneously from the BiostampRC and Bagnoli sensors which were placed next to each other above the biceps brachii muscle, 1/3 of the distance from the fossa cubit to the medial acromion, in accordance with the SENIAM recommendations [16]. The biceps brachii was chosen due to the relatively large size and simple architecture of the muscle, and limited contribution of cross-talk from surrounding muscles to the surface EMG signal. IEDs were fixed at 45 mm for BiostampRC and 10 mm for Bagnoli, see Table 1. For Bagnoli, a reference electrode was also placed on the skin above the subject's olecranon fossa, Fig. 1. Differences in sensor properties, such as IED and electrode surface area, are summarized in Table 1 and addressed in Section IV.

C. Sampling rates

The sampling rate for Bagnoli was set to 2174 Hz throughout the protocol.

Due to the large inter-electrode distance of BiostampRC, reduced frequency content of the recorded signals would be expected. As the lowest available sampling rate that satisfies the Nyquist criterion is desirable for sensors where data are stored on board the sensor or streamed, data recorded with the wearable sensor using the two highest available sampling rates (500 Hz and 1000 Hz) were first examined. BiostampRC data were collected from the biceps brachii muscle of a single subject during a series of 5 s isometric contractions at 30% MVC. Twenty contractions were performed, ten at each sampling rate. A rest period of at least one minute was provided between each contraction. The EMG power spectra were analyzed and the median frequency was calculated for all contractions at both sampling rates and compared using two-sample t-tests. The distribution of the signal power was similar for both sampling rates, with no significant difference in median frequency at the two sampling rates observed ($p = 0.33$). The BiostampRC data were, therefore, subsequently sampled at the lower rate of 500 Hz.

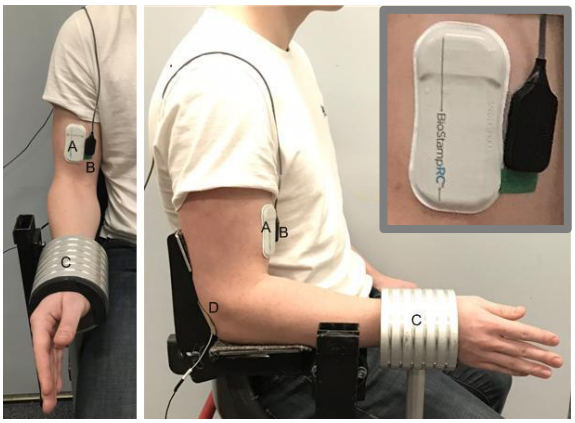

Fig 1. Front (left) and side (right) views of experimental set up. A: BiostampRC, B: Bagnoli, C: cuff, D: reference electrode. Inset (top right) depicts close up view of both sensors.

Table 1. Summary of EMG system configurations.

Sensor name	Bagnoli	BiostampRC
Manufacturer	Delsys Inc.	MC10 Inc.
Wearable	No	Yes
Wired/Wireless	Wired	Wireless
Sampling rate	2174 Hz	500/1000 Hz
Inter-electrode distance	10 mm	45 mm
Electrode shape	Rectangular x2	Circular x4
Electrode dimensions	1 x 10 mm	Diameter = 10mm
Sensor dimensions (LxWxH)	41x20x5 mm	66x34x4.5 mm
Resolution	16 bit	16 bit
Electrode Material	99.9% Ag	Ag/AgCl
Data storage	N/A	On-board memory 32MB
Data transfer	N/A	Bluetooth

D. Validation protocol

To minimize the effect of electrode placement on EMG amplitude, a counterbalanced design was used [29]. This involved placing the BiostampRC electrode lateral to the Bagnoli electrode in six subjects, and the Bagnoli system lateral to the BiostampRC system in the remaining six subjects. The skin was prepared by gentle abrasion and with the use of alcohol swabs. Electrode gel was used for both systems.

Subjects initially performed two 5 s maximum voluntary contractions (MVCs). The first and last second of data were excluded, and the mean resultant force was calculated over the remainder of each MVC. The mean value of the two iterations was used as the final MVC value for each subject. Following this, each subject performed submaximal isometric contractions ranging from 10% to 80% MVC, at 10% intervals and in a random order. Subjects were required to maintain each contraction for 5 s and to complete the series twice, yielding 16 submaximal isometric contractions per subject. The first and last second of data were excluded, and all EMG features were calculated using the remainder of each contraction.

Each subject was then asked to hold a sustained fatiguing contraction at 30% MVC until their force decreased below 10% of the target force value and remained at or below this level for 5 s. Rest periods of at least one minute were provided between MVC and submaximal contractions, between submaximal contractions and before the fatiguing contraction.

E. Data analysis

Data were analyzed using custom developed algorithms in MATLAB (The MathWorks, Inc, Natick, MA). Bagnoli and BiostampRC data were bandpass filtered between 20-250 Hz and 20-450 Hz, respectively, using a 6th order Butterworth filter. Data were manually annotated into sections of EMG activity and non-EMG data recorded during quiescent periods between contractions. The baseline noise for each system was calculated as the root mean square (RMS) amplitude of the quiescent data for all periods.

On inspection of the raw sensor data (Fig. 2B and 2D), a signal artefact was observed in the BiostampRC data at regular intervals of 122 samples (approximately 4.1 Hz for a sampling rate of 500 Hz), corresponding to instances when data were written to the flash ROM [30]. A template subtraction algorithm was used to minimize the impact of this artefact on the BiostampRC data, using an approach similar to that used to remove artefacts from known sources from EMG signals, including ECG [31], [32] or stimulus artefacts [33], [34]. As the amplitude of the signal artefact was observed to vary gradually over time, the template was adapted for each data section. Within each active EMG and quiescent period, data were divided into non-overlapping epochs of 122 samples. During each quiescent period, a template was created by calculating the mean of all epochs in that section, and then subtracted from the corresponding data section. For each section of EMG data, the mean of the templates for the two adjacent quiescent periods was estimated and subtracted from the corresponding EMG section. Following this template subtraction routine, baseline noise was recalculated.

The onset of a muscle contraction and EMG onset and offset times were automatically detected using the Teager-Kaiser energy (TKE) method [17]. The method utilizes the TKE operator which is sensitive to changes in the instantaneous amplitude and frequency of the signal [35]. Where EMG activity was detected, EMG onset and offset times were estimated and the percentage of submaximal contractions correctly detected was computed.

The RMS amplitudes of the EMG signals from each system were calculated using a 500 ms moving window with 250 ms overlap and normalized with respect to the RMS amplitude at 100% MVC. The RMS amplitude of each 5 s isometric contraction was estimated as the mean RMS amplitude from the middle 3 s of each contraction.

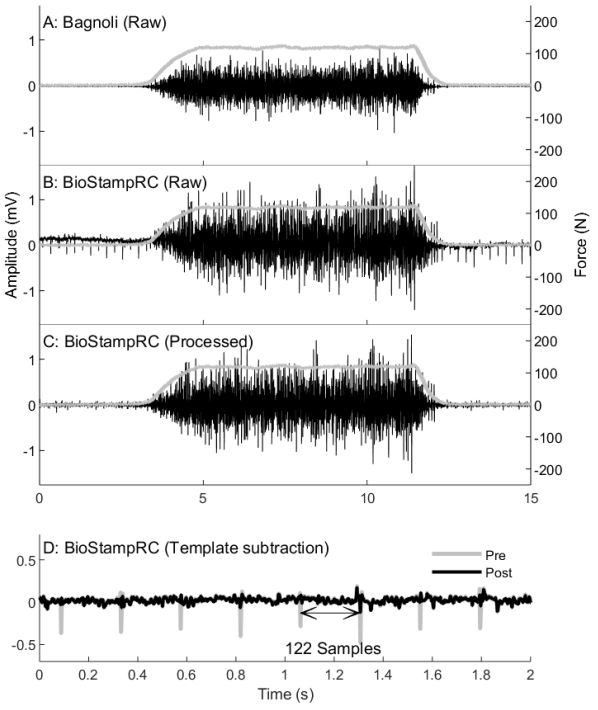

Fig. 2. Sample EMG data recorded during a 70% MVC contraction for a representative subject. A and B: A 15 s sample of raw data recorded by the Bagnoli and BiostampRC EMG electrodes. C: BiostampRC data (A) after filtering and template subtraction. D: Example of 2 s of quiescent BiostampRC data before (pre) and after (post) template subtraction, illustrating the observed signal artefact. Force recorded by the load cell under the wrist is superimposed in subplots A-C in grey.

The median frequency of the EMG power spectra were then estimated [19], and normalized to the median frequency for each subject's MVC. Two nonlinear features which measure the degree of hidden complexity and regularity in the structure of the EMG signal were also estimated – percentage determinism [36] and multiscale entropy [37].

To examine the relative change in EMG median frequency during the fatiguing contraction, the data were divided into segments representing 10% of the time from the start of the contraction to task failure. The median frequency for each 10% time segment was estimated as the median value of the median frequencies calculated for non-overlapping 5 s duration windows. The median frequency at each point was then normalized with respect to the initial value for that subject.

To estimate the non-linear features percentage determinism and multiscale entropy, data recorded using the Bagnoli and BiostampRC systems were downsampled and upsampled, respectively, to 1000 Hz. To estimate the percentage determinism, a multidimensional phase space was reconstructed from time-delayed state vectors (embedding dimension = 15, time-delay = 1) [21]. The Euclidean distance between all states was calculated and a finite number of neighbors approach (# neighbors = 5) was used to compose the recurrence plot [38]. Percentage determinism was determined from the recurrence plot as the number of consecutive pixels forming diagonal lines of 10 or more [21]. At each force level, percentage determinism was computed using the middle 3 s of EMG data. For the fatiguing contractions, the initial and final 3 s of data were excluded, and the percentage determinism was calculated using the first and last 3 s of the remaining signal, and 3 s of data centered midway through the contraction. Sample recurrence plots for a representative subject are presented in Fig. 3.

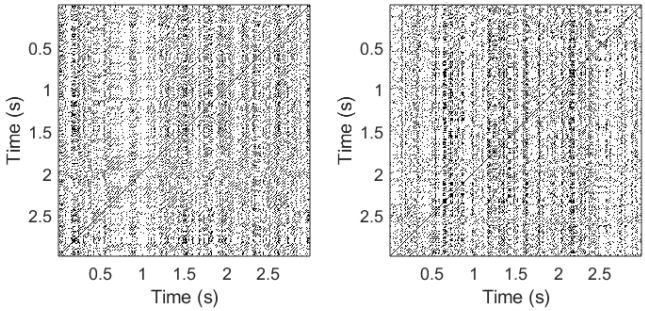

Fig. 3. Sample recurrence plots for a contraction at 80% MVC for a representative subject. The percentage determinism for the data presented was 37.86 % (BiostampRC - left) and 25.08 % (Bagnoli - right).

To estimate multiscale entropy, sample entropy was estimated at increasing time scales, and the complexity index was calculated as the area under the curve of time scale versus sample entropy [37], Fig. 4. For all contraction conditions, the template sequence length, *m*, was set to 3, and the matching threshold set at 20% of the signal standard deviation [37]. Based on theoretical considerations, a minimum signal length of 10^m has been recommended for estimation of approximate and sample entropy [39]. A maximum time scale of 5 was thus chosen for all contractions based on the maximum signal length available. For a sampling rate of 1 kHz, a time scale of 4 corresponds to a period of 4 ms between consecutive points in the template sequence, equivalent to estimating the sample entropy at a time scale of 8 at 2 kHz, 2 at 500 Hz or 1 at a sampling rate of 250 Hz (Fig. S1). At each force level, the complexity index was computed using 4.5 s of EMG data centered on the middle of the contraction to optimize the amount of data available for analysis. For the fatiguing contractions, the initial and final 4.5 s of data were excluded, and the complexity index was calculated using the first and last 4.5 s of the remaining signal, and 4.5 s of data centered at the middle of the contraction.

To minimize the influence of inter-subject variance on the graphical representation of the results for force-varying contractions (Figures 5-8), data for each subject were normalized by subtracting that subject's mean value over all force levels and adding on the grand mean over all subjects [40], [41].

F. Statistical analysis

The baseline noise, EMG onset and offset times, and contraction durations for each system were compared using two-tailed paired t-tests.

Two-way, within subject repeated measures ANOVA was used to test for differences between the two EMG systems. For analysis of RMS amplitude, median frequency, percentage determinism and complexity index, the within-subject factors were the EMG system (BiostampRC or Bagnoli) and contraction intensity or time.

To compare the rate of decay of the EMG median frequency during the fatiguing contractions, the slope and the intercept of a linear fit of the median frequency during the fatiguing contraction were calculated for each subject [42]. Paired t-tests were performed on the slopes of the lines and the intercepts for the two systems. A significance level of $\alpha = 0.05$ was used for all statistical tests.

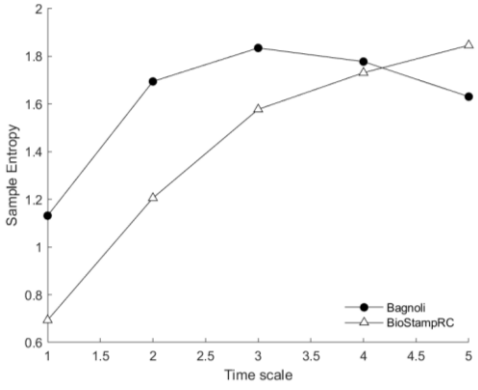

Fig. 4. Example of sample entropy curves for EMG signals recorded using the BiostampRC and Bagnoli sensors for a contraction at 80% MVC for a representative subject.

III. RESULTS

Sample EMG data recorded during a single isometric contraction at 70% MVC for Bagnoli and BiostampRC are presented in Fig. 2. Prior to template subtraction, BiostampRC had significantly higher baseline noise (0.039 ± 0.018 mV)

compared to Bagnoli (0.011 ± 0.012 mV), $p < 0.001$ (Fig. 2). While the baseline noise for BiostampRC reduced following template subtraction to 0.029 ± 0.021 mV (Fig. 2C), it remained significantly greater than Bagnoli ($p=0.015$).

The Teager-Kaiser energy method successfully identified the onset and offset of 89% and 96% of the submaximal contractions for the BiostampRC and Bagnoli EMG data, respectively, with all of the unidentified contractions being either at 10% or 20% MVC. Estimated EMG onset and offset times, and contraction durations, did not significantly vary between EMG systems ($p = 0.34$, $p = 0.77$, and $p = 0.64$, respectively).

A. Force-varying contractions

Normalized RMS amplitude significantly increased with increasing force during the isometric contractions, as expected ($p < 0.001$), Fig. 5. This relationship did not vary between EMG systems ($p = 0.55$), and there was no significant interaction between force level and EMG system ($p = 0.96$).

Absolute and normalized median frequency both significantly increased with force ($p < 0.001$ for both), Fig. 6. A significant difference between EMG systems was observed for both the absolute and normalized median frequency ($p < 0.001$ and $p = 0.017$ respectively), Fig. 6. The interaction between EMG system and force level was also significant for both absolute and normalized median frequency ($p < 0.001$ for both), Fig. 6.

As force increased, a significant reduction in percentage determinism ($p < 0.001$, Fig. 7), and a significant increase in complexity index ($p = 0.019$, Fig. 8) was observed. Percentage determinism was significantly different for EMG signals recorded using BiostampRC and Bagnoli ($p < 0.001$). Complexity index also varied significantly between EMG systems ($p = 0.002$), with higher percentage determinism and lower entropy observed for BiostampRC relative to Bagnoli. The interaction between EMG system and force was significant for complexity index ($p = 0.04$) but not percentage determinism ($p = 0.54$).

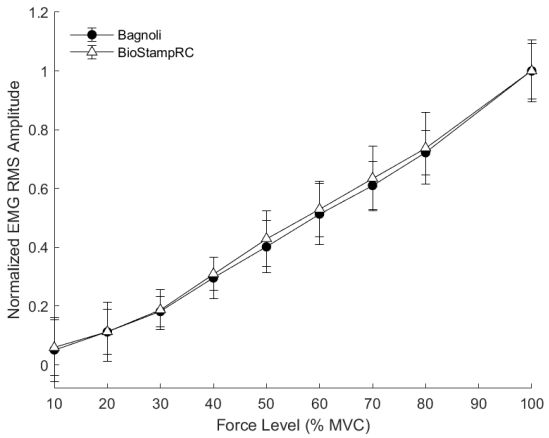

Fig. 5. Force level (% MVC) versus normalized EMG amplitude for both EMG systems. The mean and SD of all data are presented.

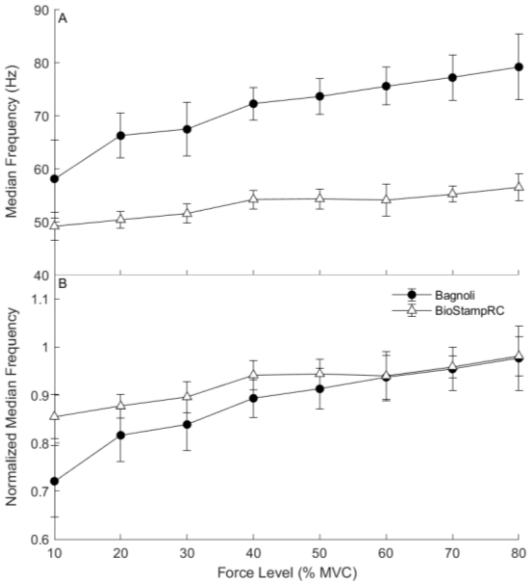

Fig. 6. Force level (% MVC) versus (A) EMG median frequency (Hz), and (B) median frequency normalized to the median frequency at 100% MVC for each subject and EMG system. The mean and SD of all subject data are presented.

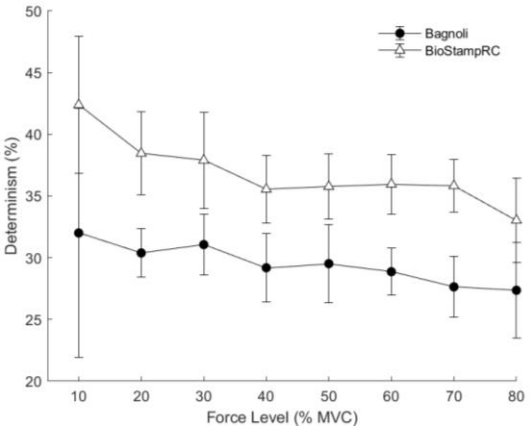

Fig. 7. Force (% MVC) versus percentage determinism for both EMG systems. The mean and standard deviation of all subject data are presented.

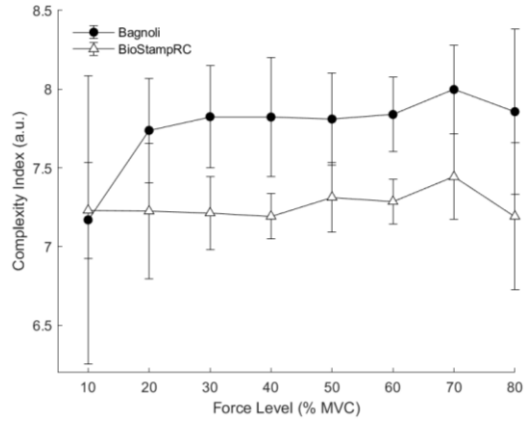

Fig. 8. Force level (% MVC) versus Complexity Index for both EMG systems. The mean and standard deviation of all data are presented.

B. Fatiguing contractions

The mean time to fatigue for all subjects was 269.1 ± 228.3 s (range: 94.0 to 927.0 s) for Bagnoli, and 273.5 ± 226.7 s

(range: 113.0 to 927.1 s), for BiostampRC. The estimated time to fatigue did not vary between EMG systems (p=0.96).

Normalized RMS amplitude increased progressively during the fatiguing contraction ($p < 0.001$), while normalized median frequency decreased ($p < 0.001$), for both systems, Fig. 9B. Neither EMG system, nor the interaction between time and EMG system, significantly affected either the change in RMS amplitude ($p = 0.57$ and $p = 0.85$) or the normalized median frequency ($p = 0.11$ and $p = 0.27$).

The mean rate of change in absolute median frequency, or slope, for all subjects was -6.55± 5.4 Hz/s for BiostampRC and -6.90 ± 14.3 Hz/s for Bagnoli ($p = 0.92$). The intercept of the lines was significantly lower for BiostampRC (52.22 ± 5.51 Hz) compared with Bagnoli (71.09 ± 13.26 Hz), confirming lower initial median frequency values for BiostampRC ($p < 0.001$), observed also in the force-varying contractions.

Percentage determinism increased during the fatiguing contractions ($p < 0.001$), and was significantly greater for BiostampRC compared with Bagnoli ($p < 0.001$), Fig. 10A. Conversely, CI decreased during the fatiguing contractions ($p < 0.001$), and was significantly less for BiostampRC compared with Bagnoli ($p < 0.01$), Fig. 10B. The interaction between sensor type and time was not significant for percentage determinism or complexity index.

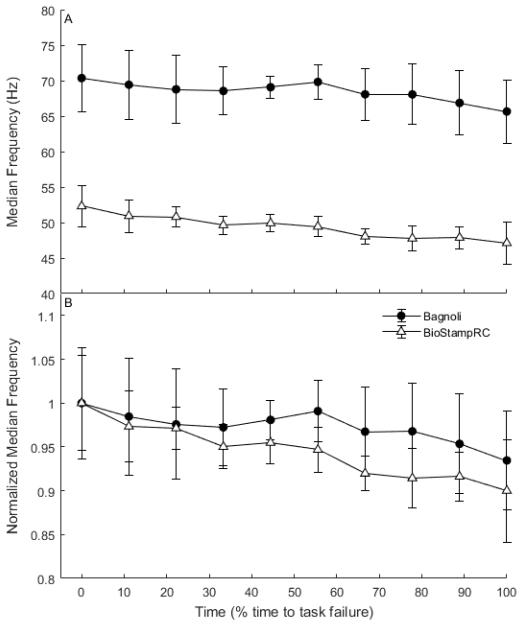

Fig. 9. The relationship between time to task failure (%) and median frequency (A), and median frequency normalized to the initial value for each subject (B) during the fatiguing contraction.

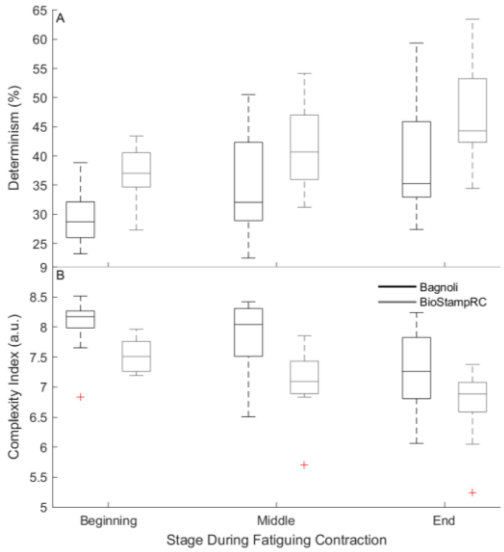

Fig. 10. Boxplots representing A: percentage determinism and B: multiscale entropy at the start, middle and end of the fatiguing contraction.

IV. Discussion

Recent developments in wearable EMG sensors open new possibilities to continuously monitor muscle activity during daily living [1]–[5]. Understanding how sensor design influences the behavior of widely used EMG features under controlled isometric conditions is an essential first step before applying these systems to more complex dynamic movements in more challenging environments. In this study, the features of surface EMG signals recorded using a wireless and wearable sensor were compared with a reference laboratory system during a series of force-varying and fatiguing isometric contractions.

A. Sensor Properties

The wearable sensor, BiostampRC, is a flexible, unobtrusive, waterproof sensor that offers the potential for continuous recording of surface EMG outside of the laboratory. Due to the sensor design, the properties deviate in several aspects from conventional research-grade EMG recording systems.

In particular, the 45 mm inter-electrode distance of the test sensor is larger than that generally recommended for bipolar surface EMG. It has been well-established through theoretical, experimental and simulation studies that the frequency content of the surface EMG signal decreases with increasing inter-electrode distance due to increased detection volume and reduced spatial filtering of the signal [22]–[27]. The lower frequency content of the EMG signals detected with BiostampRC, reflected in lower median frequencies, are, therefore, as expected and consistent with previous studies on the influence of electrode configuration, Fig. 6 and Fig. 9.

To reduce memory requirements and optimize battery life for long-term recording it is desirable to minimize sampling rate, while preserving the signal features. In preliminary analysis, the effect of sampling rate on the BiostampRC signals was examined, confirming that reducing the sampling frequency from 1 kHz to 500 Hz did not alter the EMG power spectrum or median frequency, as the frequency content lay below 250 Hz.

This is lower than the frequency content of typical bipolar surface EMG signals which is generally assumed to lie between approximately 10 and 500 Hz, with the highest frequency components varying depending on the inter-electrode distance, subcutaneous tissue thickness and muscle examined. While the lower sampling rate did not influence the data recorded in this case, with smaller inter-electrode distances or above muscles with less subcutaneous tissue where the electrode lies closer to the muscle fibers this could result in under-sampling of the surface EMG signal.

Differences in electrode shape and orientation also influence the voltage detected at the electrode, which approximates the mean value of the extracellular potential at the skin surface directly beneath the electrode [43]. Electrode impedance differs with surface area, which could further affect signal quality. The larger size of the BiostampRC electrode in the direction parallel to the muscle fibers would be expected to have an integrative effect on the data, decreasing further high frequency content [44], which may also contribute to the lower median frequencies observed for the wearable sensor.

Baseline noise was higher for the wearable sensors compared with the Bagnoli standard laboratory system, Fig. 2. This noise included an artefact due to electromagnetic signal coupling between the analog signal traces and the flash ROM data traces, which are closely routed in the sensor's circuitry [30]. The noise level reduced following artefact removal, but remained significantly higher than that of the reference system.

The influence of differences in the sensor properties on features commonly used to quantify EMG amplitude, spectral distribution, deterministic structure and complexity, during force-varying and fatiguing isometric contractions, is discussed below.

B. RMS Amplitude and Median Frequency

Both EMG systems exhibited the well-established non-linear force-EMG relationship for the biceps brachii [45], [46], Fig. 5, with no significant difference observed between the two systems. EMG median frequency increased with increasing force, Fig. 6, consistent with previous studies and generally attributed to the recruitment of motor units with higher conduction velocities at higher contraction levels [47]. The relationship between EMG median frequency (both absolute and normalized) and force was found to be significantly different between the two systems.

A higher sensitivity of spectral indices to changes in force has been reported for electrodes with smaller inter-electrode distances in certain muscles, consistent with the lower sensitivity of the median frequency observed for the wearable system here, Fig. 6 [45], [48]. In addition to the influence of inter-electrode distance, the relationship between force and median frequency in the BiostampRC may be further influenced by the higher noise levels observed for the BiostampRC which may have contributed to an artificial increase in estimated median frequencies at lower force levels, Fig. 6A.

Both systems also exhibited the characteristic progressive increase in EMG amplitude and reduction in EMG median frequency during the sustained fatiguing contraction, as expected, Fig. 9. While absolute values were different between systems, the rate of change of both the EMG RMS amplitude and normalized EMG median frequency with fatigue was not significantly different.

C. Surface EMG Determinism and Spectral Complexity

The percentage determinism decreased while signal complexity, assessed using the complexity index, increased with increasing force for both EMG systems, Fig. 7 and Fig. 8. The complexity of the EMG signal recorded using the BiostampRC was less sensitive to changes with force than that of the EMG signals recorded using the laboratory system.

Previous studies have reported an increase in the surface EMG signal complexity with increasing contraction intensity [18], [49], consistent with Fig. 7 and Fig. 8. As the number of motor units recruited and their firing rates increase with contraction intensity, the structure of the EMG signal becomes more random due to increased superposition of uncorrelated motor unit action potential trains during the transition from low to higher forces [50]. Percentage determinism could thus be expected to decrease with increasing contractile force and surface EMG signal density, and complexity to increase.

The estimated percentage determinism was greater for the BiostampRC than for the Bagnoli sensor at all force levels, and during the fatiguing contraction. This was mirrored by lower complexity index values at all force levels and during the fatiguing contraction for the BiostampRC. The difference in complexity measures for the two sensors may be due to the lower frequency content of the BiostampRC and reduced contribution of higher frequency components which are more random in structure. The sensitivity of the percentage determinism to detect nonlinear changes in the surface EMG signal due to fatigue has been well documented [18], [20], [36], [51]. This result is reflected here with the percentage determinism increasing progressively during the fatiguing contraction for both electrodes.

D. Limitations

The inter-electrode distance, hardware filtering and sampling rates of the reference electrode were representative of those typically used to record surface EMG in the laboratory environment and complied with the SENIAM guidelines for surface EMG recording. Comparison with electrodes of varying inter-electrode distances and shape may yield additional comparative insights. The results presented here were limited to isometric conditions in a relatively small group of primarily younger healthy subjects, without considering changes associated with aging or pathological conditions. To minimize the effect of electrode placement on the resultant EMG data, a counterbalanced design was used, however the effect of electrode placement on the reported EMG features was not statistically examined. The features of the surface EMG signal and changes with increasing force and fatigue may differ across muscles, with subject anatomy and subcutaneous fat thickness. In particular, the tissue between the electrode and muscle fibers has a spatial low pass filtering effect on the EMG signal detected at the skin surface, which decreases both the amplitude

and frequency content of the signal [52]. Dynamic contractions occurring during complex free-living movements, far from the laboratory set up, will also pose additional challenges due to motion artefact, movement of the electrode and muscle fibers relative to one another and variations in the geometry of the surrounding volume conductor. Additionally, the effects of variables such as ambient temperature and temperature at the electrode-tissue interface on sensor performance were not examined. Despite these limitations, establishing signal properties under isometric conditions in healthy subjects is a critical first step before progressing to a wider range of conditions.

V. Conclusion

The advent of wireless wearable EMG sensors opens the possibility of continuous monitoring of muscle activity during everyday life. Reliable long-term recording of high quality EMG signals with unobtrusive sensors under these conditions is challenging and currently requires compromises in sensor design with respect to the laboratory gold standards. Understanding how these factors affect the resultant EMG signals is critical before this new generation of sensors can be fully utilized. In this study, a wireless, wearable EMG sensor was compared against a standard wired laboratory reference during a series of force-varying and fatiguing isometric contractions. The results indicate that the wearable sensor, BiostampRC, can accurately detect EMG onset and offset times, and changes in EMG amplitude during fatiguing and non-fatiguing isometric contraction, despite a relatively large inter-electrode distance, lower sampling rate and higher baseline noise than comparable laboratory systems. However, differences in EMG spectral features, specifically the EMG median frequency, and nonlinear complexity measures were observed between signals recorded by the wearable sensor compared and a laboratory reference system. These differences are likely due to a reduction in higher frequency EMG components due to the larger inter-electrode distance and lower sampling frequency of the wearable sensor.

References

[1] P. Bonato, “Wearable sensors/systems and their impact on biomedical engineering,” *IEEE Eng. Med. Biol. Mag.*, vol. 22, no. 3, pp. 18–20, 2003.

[2] I. Mazzetta, A. Zampogna, A. Suppa, A. Gumiero, M. Pessione, and F. Irrera, “Wearable Sensors System for an Improved Analysis of Freezing of Gait in Parkinson’s Disease Using Electromyography and Inertial Signals,” *Sensors*, vol. 19, no. 4, 2019.

[3] I. Mazzetta *et al.*, “Stand-Alone Wearable System for Ubiquitous Real-Time Monitoring of Muscle Activation Potentials,” *Sensors*, vol. 18, no. 6, 2018.

[4] Y. Athavale and S. Krishnan, “Biosignal monitoring using wearables: Observations and opportunities,” *Biomed. Signal Process. Control*, vol. 38, no. Supplement C, pp. 22–33, 2017.

[5] G. Biagetti, P. Crippa, L. Falaschetti, S. Orcioni, and C. Turchetti, “Human activity monitoring system based on wearable sEMG and accelerometer wireless sensor nodes,” *Biomed. Eng. Online*, vol. 17, 2018.

[6] A. Burns *et al.*, “SHIMMER™: an extensible platform for physiological signal capture,” in *Engineering in Medicine and Biology Society (EMBC), 2010 Annual International Conference of the IEEE*, 2010, pp. 3759–3762.

[7] M. M. Kabir, E. A. Perez-Alday, J. Thomas, G. Sedaghat, and L. G. Tereshchenko, “Optimal configuration of adhesive ECG patches suitable for long-term monitoring of a vectorcardiogram,” *J. Electrocardiol.*, vol. 50, no. 3, pp. 342–348, 2017.

[8] Y. Moon *et al.*, “Monitoring gait in multiple sclerosis with novel wearable motion sensors,” *PLoS One*, vol. 12, no. 2, p. e0171346, 2017.

[9] J. L. Adams *et al.*, “Multiple Wearable Sensors in Parkinson and Huntington Disease Individuals: A Pilot Study in Clinic and at Home,” *Digit. Biomarkers*, vol. 1, no. 1, pp. 52–63, 2017.

[10] R. S. McGinnis *et al.*, “Wearable sensors capture differences in muscle activity and gait patterns during daily activity in patients recovering from ACL reconstruction,” in *2018 IEEE 15th International Conference on Wearable and Implantable Body Sensor Networks (BSN)*, 2018, pp. 38–41.

[11] E. K. Pissadaki *et al.*, “Decomposition of complex movements into primitives for Parkinson’s disease assessment,” *IBM J. Res. Dev.*, vol. 62, no. 1, pp. 5:1-5:11, 2018.

[12] E. Jortberg *et al.*, “A novel adhesive biosensor system for detecting respiration, cardiac, and limb movement signals during sleep: validation with polysomnography,” *Nat Sci Sleep*, vol. 10, pp. 397–408, 2018.

[13] K. M. Chang, S. H. Liu, and X. H. Wu, “A wireless sEMG recording system and its application to muscle fatigue detection,” *Sensors*, 2012.

[14] O. M. Giggins, U. M. Persson, and B. Caulfield, “Biofeedback in rehabilitation.(Review)(Report),” *J. Neuroeng. Rehabil.*, 2013.

[15] I. Moon, M. Lee, J. Chu, and M. Mun, “Wearable EMG-based HCI for electric-powered wheelchair users with motor disabilities,” in *Proceedings - IEEE International Conference on Robotics and Automation*, 2005.

[16] H. J. Hermens *et al.*, “SENIAM 8, European Recommendations for Surface Electromyography,” *Ross. Res. Dev.*, 1999.

[17] X. Li, P. Zhou, and A. S. Aruin, “Teager-Kaiser energy operation of surface EMG improves muscle activity onset detection,” *Ann. Biomed. Eng.*, vol. 35, no. 9, pp. 1532–1538, 2007.

[18] J. G. A. Cashaback, T. Cluff, and J. R. Potvin, “Muscle fatigue and contraction intensity modulates the complexity of surface electromyography,” *J. Electromyogr. Kinesiol.*, vol. 23, no. 1, pp. 78–83, 2013.

[19] M. Lowery, P. Nolan, and M. O’Malley, “Electromyogram median frequency, spectral compression and muscle fibre conduction velocity during sustained sub-maximal contraction of the brachioradialis muscle,” *J. Electromyogr. Kinesiol.*, vol. 12, no. 2, pp. 111–118, 2002.

[20] C. Morana, S. Ramdani, S. Perrey, and A. Varray, “Recurrence quantification analysis of surface electromyographic signal: Sensitivity to potentiation and neuromuscular fatigue,” *J. Neurosci. Methods*, vol. 177, no. 1, pp. 73–79, 2009.

[21] M. W. Flood, B. R. Jensen, A. S. Malling, and M. M. Lowery, “Increased EMG intermuscular coherence and reduced signal complexity in Parkinson’s disease,” *Clin Neurophysiol*, vol. 130, no. 2, pp. 259–269, 2019.

[22] R. Merletti, D. Farina, and M. Gazzoni, “The linear electrode array: a useful tool with many applications,” *J. Electromyogr. Kinesiol.*, vol. 13, no. 1, pp. 37–47, 2003.

[23] M. M. Lowery, C. L. Vaughan, P. J. Nolan, and M. J. O’Malley, “Spectral compression of the electromyographic signal due to decreasing muscle fiber conduction velocity,” *IEEE Trans. Rehabil. Eng.*, vol. 8, no. 3, pp. 353–361, 2000.

[24] L. H. Lindstrom and R. I. Magnusson, “Interpretation of Myoelectric Power Spectra - Model and Its Applications,” *Proc. Ieee*, vol. 65, no. 5, pp. 653–662, 1977.

[25] A. J. Fuglevand, D. A. Winter, A. E. Patla, and D. Stashuk, “Detection of motor unit action potentials with surface electrodes: influence of electrode size and spacing,” *Biol Cybern*, vol. 67, no. 2, pp. 143–153, 1992.

[26] P. A. Parker and R. N. Scott, “Statistics of the myoelectric signal from monopolar and bypolar electrodes,” *Med Biol Eng*, vol. 11, no. 5, pp. 591–596, 1973.

[27] J. Rodriguez-falces, D. Neyroud, and N. Place, “Influence of inter-electrode distance, contraction type, and muscle on the relationship between the sEMG power spectrum and contraction force,” *Eur. J. Appl. Physiol. Heidelb.*, vol. 115, no. 3, pp. 627–638, 2015.

[28] T. Kleiber, L. Kunz, and C. Disselhorst-Klug, “Muscular coordination of biceps brachii and brachioradialis in elbow flexion with respect to hand position,” *Front. Physiol.*, 2015.

[29] T. J. Walters, K. A. Kaschinske, S. J. Strath, A. M. Swartz, and K.

G. Keenan, “Validation of a portable EMG device to assess muscle activity during free-living situations,” *J. Electromyogr. Kinesiol.*, vol. 23, no. 5, pp. 1012–1019, 2013.
[30] M. Support, “Personal correspondence with the author.” 2018.
[31] A. Bartolo, R. R. Dzwonczyk, C. Roberts, and E. Goldman, “Description and validation of a technique for the removal of ECG contamination from diaphragmatic EMG signal,” *Med. Biol. Eng. Comput.*, 1996.
[32] Ping Zhou, M. M. Lowery, R. F. Weir, and T. A. Kuiken, “Elimination of ECG Artifacts from Myoelectric Prosthesis Control Signals Developed by Targeted Muscle Reinnervation,” 2006.
[33] A. E. Hines, P. E. Crago, G. J. Chapman, and C. Billian, “Stimulus artifact removal in EMG from muscles adjacent to stimulated muscles,” *J. Neurosci. Methods*, 1996.
[34] K. Limnuson, H. Lu, H. J. Chiel, and P. Mohseni, “Real-time stimulus artifact rejection via template subtraction,” *IEEE Trans. Biomed. Circuits Syst.*, 2014.
[35] J. F. Kaiser, “On a simple algorithm to calculate the ‘energy’ of a signal,” *Acoust. Speech, Signal Process. 1990. ICASSP-90., 1990 Int. Conf.*, 1990.
[36] C. L. Webber, M. A. Schmidt, and J. M. Walsh, “Influence of Isometric Loading on Biceps Emg Dynamics as Assessed by Linear and Nonlinear Tools,” *J. Appl. Physiol.*, vol. 78, no. 3, pp. 814–822, 1995.
[37] M. Costa, A. L. Goldberger, and C. K. Peng, “Multiscale entropy analysis of complex physiologic time series,” *Phys Rev Lett*, vol. 89, no. 6, 2002.
[38] N. Marwan, M. C. Romano, M. Thiel, and J. Kurths, “Recurrence plots for the analysis of complex systems,” *Phys. Reports-Review Sect. Phys. Lett.*, vol. 438, no. 5–6, pp. 237–329, 2007.
[39] J. S. Richman and J. R. Moorman, “Physiological time-series analysis using approximate and sample entropy,” *Am. J. Physiol. - Hear. Circ. Physiol.*, 2000.
[40] G. R. Loftus and M. E. J. Masson, “Using confidence intervals in within-subject designs,” *Psychon. Bull. Rev.*, vol. 1, no. 4, pp. 476–490, 1994.
[41] L. McManus, X. Hu, W. Z. Rymer, N. L. Suresh, and M. M. Lowery, “Motor Unit Activity during Fatiguing Isometric Muscle Contraction in Hemispheric Stroke Survivors,” *Front. Hum. Neurosci.*, vol. 11, 2017.
[42] A. Rainoldi, G. Galardi, L. Maderna, G. Comi, L. Lo Conte, and R. Merletti, “Repeatability of surface EMG variables during voluntary isometric contractions of the biceps brachii muscle,” *J Electromyogr Kinesiol*, vol. 9, no. 2, pp. 105–119, 1999.
[43] J. P. van Dijk, M. M. Lowery, B. G. Lapatki, and D. F. Stegeman, “Evidence of Potential Averaging over the Finite Surface of a Bioelectric Surface Electrode,” *Ann. Biomed. Eng.*, vol. 37, no. 6, pp. 1141–1151, 2009.
[44] H. J. Hermens, B. Freriks, C. Disselhorst-Klug, and G. Rau, “Development of recommendations for SEMG sensors and sensor placement procedures,” *J. Electromyogr. Kinesiol.*, vol. 10, no. 5, pp. 361–374, 2000.
[45] J. H. Lawrence and C. J. De Luca, “Myoelectric signal versus force relationship in different human muscles,” *J. Appl. Physiol.*, vol. 54, no. 6, pp. 1653–1659, 1983.
[46] E. P. Doheny, T. G. Foran, and B. R. Greene, “A single gyroscope method for spatial gait analysis,” in *Engineering in Medicine and Biology Society (EMBC), 2010 Annual International Conference of the IEEE*, 2010, pp. 1300–1303.
[47] C. J. De Luca, L. Donald Gilmore, M. Kuznetsov, and S. H. Roy, “Filtering the surface EMG signal: Movement artifact and baseline noise contamination,” *J. Biomech.*, vol. 43, no. 8, pp. 1573–1579, 2010.
[48] T. Moritani and M. Muro, “Motor unit activity and surface electromyogram power spectrum during increasing force of contraction,” *Eur J Appl Physiol Occup Physiol*, vol. 56, no. 3, pp. 260–265, 1987.
[49] R. Istenic, P. A. Kaplanis, C. S. Pattichis, and D. Zazula, “Multiscale entropy-based approach to automated surface EMG classification of neuromuscular disorders,” *Med. Biol. Eng. Comput.*, vol. 48, no. 8, pp. 773–781, 2010.
[50] M. M. Lowery and M. J. O’Malley, “Analysis and Simulation of changes in EMG amplitude during high-level fatiguing contractions,” *IEEE Trans. Biomed. Eng.*, vol. 50, no. 9, pp. 1052–1062, 2003.
[51] G. C. Filligoi and F. Felici, “Detection of hidden rhythms in surface EMG signals with a nonlinear time-series tool,” *Med. Eng. Phys.*, vol. 21, no. 6–7, pp. 439–448, 1999.
[52] M. M. Lowery, N. S. Stoykov, and T. A. Kuiken, “Independence of myoelectric control signals examined using a surface EMG model,” *IEEE Trans. Biomed. Eng.*, 2003.